Classification of Bone Fracture Widths using CST-based Microwave Imaging Simulations

Ebenezer Adjei[1], Prince O. Siaw[1], Joaquim M.C.S. Bastos[1,2], Ahmad Aldelemy[1]

{e.adjei@bradford.ac.uk: p.o.siaw@bradford.ac.uk: jbastos@av.it.pt: a.a.aldelemy@bradford.ac.uk}

[1]Biomedical and Electronic Engineering, University of Bradford, Bradford, BD7 1DP, UK
[2]The Instituto de Telecomunicações, Campus Universitário de Santiago, Aveiro 3810-193, Portugal

Abstract. Human fracture has gained much popularity in the healthcare system due to its high rate of occurrences via conditions such as osteoporosis, accidents, and pressure exertion, particularly in the aged population. In this research, a low-cost and non-invasive microwave sensor technique is proposed as a medical imaging technique for bone fracture detection. A frequency range of 1 – 3 GHz for a patch antenna was designed for this research. The sensor was used to detect fracture depths of 0.2mm, 0.5mm, 1mm, and 2mm. The findings were compared to the S-parameter of the antenna when tested in free space and a bone without fracture. The results obtained from the S–S-parameter proved the concept of using the microwave sensor technique as an alternate cost-effective method in human fracture detection.

Keywords: Fracture, Monopole Antenna, Microwave imaging, S-Parameter, Fairfield, Bone phantom, Hematoma, CST modelling.

1. Introduction

Bone fractures are notably common and often devastating medical conditions causing distress to millions of people globally. An accurate assessment and classification of these fractures are vital for predicting patient outcomes and administering suitable treatments. Predicting the severity of bone fracture and guiding the course of medical intervention makes the ability to understand the depth of fracture pivotal [1]. Although conventional methods such as the X-ray, computed tomography (CT) scan, and MRI have proven essential in achieving such milestones, the limitations associated with them such as radiation exposure and the complexity of this equipment have necessitated the need to resort to simple non-invasive and less costly approaches [2].

For many years, different medical imaging techniques such as X-ray, magnetic resonance imaging (MRI), and computed tomography (CT) scans have been the source for bone fracture detections, with X-ray being the most predominant technique widely employed although MRI has proven to provide better contrasts between the bone and its associated tissues such as the muscle, bone marrow, and other soft tissues. These imaging techniques continue to be of great to humanity and the healthcare system. However, drawbacks associated with the use of these

IMDC-IST 2023, October 25-27, Yola, Nigeria

DOI 10.4108/eai.25-10-2023.2348745

conventional techniques such as patients' exposure to ionizing radiations, the high cost of using MRI technique, the invasive nature, and the ready availability have forced scientists and researchers to resort to a more innovative technique that serves a similar purpose and still overcomes these challenges [3].

In recent times, microwave imaging has gained the spotlight as the most suitable alternative to these conventional techniques for detecting early breast cancer [4], bone fracture [5], brain haemorrhage [6], brain stroke [7], and other defective tissues in the human body. Concerning bone fracture detection, several studies have been conducted to ascertain the feasibility of implementing microwave imaging as a non-invasive, non-ionizing, and less costly innovative approach for the medical imaging of bone fractures. To evaluate the feasibility of implementing MWI in medical diagnostics, several studies have been conducted. [8] and [9] MammoWave technique in a free space 3D tube model setup to detect longitudinal bone fracture and lesions.

However, image formation through the MWI technique can be very difficult due to its dependency on the dielectric contrasts of these tissues in the image reconstruction. The dielectric properties of some tissues are almost impossible to distinguish due to the close similarities in the images produced. For instance, though a large contrast is seen between fatty tissue and a cancerous breast, a very small difference is seen when the same cancerous tissue is compared to a glandular breast tissue, the detection of the cancerous in near such tissues a challenging task [10]. The purpose of this research is to develop a fracture detection system other than the conventional system capable of detecting and distinguishing variations in the degree of human fractures. In place of the usual image processing algorithm, this experiment focuses on using significant variations in the S-Parameters through the measurement of the electrical impedance of the tissues at different frequencies. the variations in the magnitude of impedance at different frequencies will serve as the baseline for the analysis of the results obtained. To comprehend the rationale behind this experiment, Table 1 demonstrates the already existing works in the areas of microwave imaging techniques for bone tissue detection, describing their techniques and the findings in each scenario.

Table 1. This shows the most recent investigations and the findings.

Reference	Investigation	Technique Used	Findings
[8]	Free-space operating microwave imaging device for bone lesion detection.	A low-complexity microwave imaging operating in free space in the 1-6.5 GHz frequency band.	A resolution of 5 mm and a signal-to-clutter ratio in a linear scale were achieved.
[11]	Sensitivity of microwave imaging for small-width bone fracture detection	Vivaldi antenna of a monostatic radar type operating in 8.3-11 GHz frequency	Proposed systems could be used in the detection of transverse bone as thin as 0.25 mm.
[12]	Fracture diagnosis of human tibia using a compact microwave device.	A planar ring resonator tested on human bone coated with porcine tissues	An average detection accuracy of 98.86% was achieved with a specific absorption rate

			below the minimum (1.6W/Kg).
[13]	Evaluation of thin bone fracture using microwave imaging.	A single small Vivaldi antenna is used on longitudinal planes of the bones.	The system could detect a fracture as low as 0.35 mm in thickness.
[14]	Microwave sensor for new approach in monitoring hip fracture healing	A non-invasive planar sensor operating in a frequency domain of 1 to 3 GHz with CESRR and ISSCR resonator was used in detecting variations in the fracture healing stages.	Better penetration characteristics were obtained by the sensors used.
[15]	Dual-polarised microwave sensor for human fracture detection.	A miniaturized dual-polarized transceiver sensor system was built adding reactive impedance surfaces.	The Reactive Impedance Surface (RIS) layer helped reduce its size by 30% and improved impedance matching compared to conventional designs, resulting in enhanced fracture detection accuracy

2. Description of System Architecture

The proposed diagnostic system comprises a patch antenna for non-invasive fracture monitoring at a frequency range of 1-3 GHz. The antenna is connected to a vector network analyser (VNA) to analyse the frequency response from the antenna by taking measurements of the S-Parameter, Impedance return loss, and gain. With the help of a computer, the sensor is controlled to obtain a desirable measurement through the VNA and resulting data is stored on the computer device for further analysis.

3. Antenna Design for Microwave Imaging System

In this research, a microwave sensor is proposed to provide medical diagnostics for human bone fracture detection. It is expected that a smaller wavelength is applied to obtain the highest resolution images as the standard requirement for medical imaging devices. Obtaining these high-resolution images requires that the chosen antenna is has a wide bandwidth, smaller in size, and has a directional radiating pattern operating in near-field mode [4]. Unfortunately, a higher frequency results in decreasing penetration depth. In the research, a frequency range of 1-3 GHz was selected for the designed sensor. Metamaterials were introduced to compensate for the overall size of the antenna. The dimensions used for this design were 18.5mm x 11mm x 1mm. Figure 1 below illustrates the dimensions used in the design of the antenna with a microstrip port. All materials used in the antenna design can be seen in Table 1.

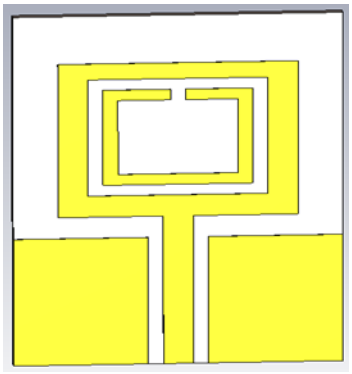

Figure 1. An image of the C*ST*-designed monopole antenn*a* represents the dimensions used in the antenna design**.**

Table 2. Represents the components of the antenna design and the material types used for each component.

Component	**Material Type**
Substrate	FR-4 (lossy)
Patch	Copper (annealed)

4. Bone Phantom Design

The human body is a complex structure with a combination of varied tissues, hence, assuming its heterogeneous nature with diverse dielectric properties. In the absence of a real human for the investigation, a bone phantom was created to mimic a real bone. The phantom created included skin, fat, muscle, and a cortical bone (comprising of the combination of the cortical bone and the marrow due to their homogeneity) as shown in Figure 2. In representing the hematoma formed when a fracture occurs in human bones, blood was used as the filler material in the fractured region of the bone. Each of these tissues was defined with their corresponding dielectric properties in Table 2 to ensure easy detection of the fractured region since it has been labelled with specific dielectric properties. Figure 2 illustrates a cylinder geometry of the proposed design to mimic the bone phantom with the dielectric properties of the applied tissues obtained at a frequency range of 1-3 GHz, whereas Figure 3, represents the RF sensor mounted on the human tissues.

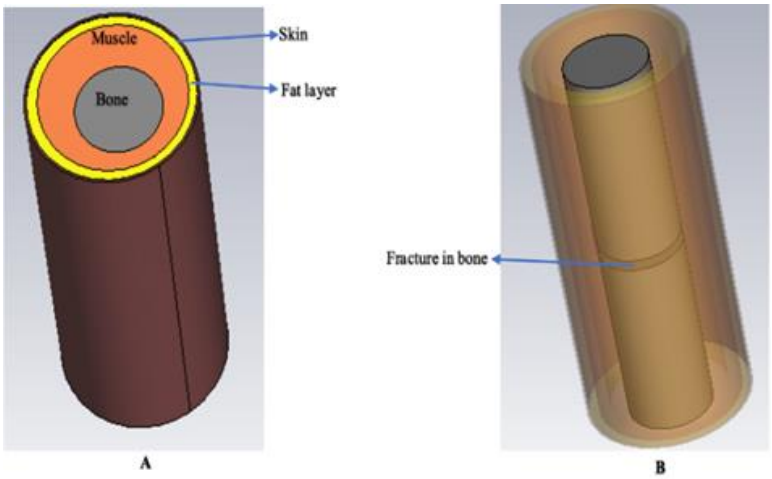

Figure 2. Cylindrical diagrams showing the bone phantom. **A** depicts the labelled phantom and **B** shows the inner phantom with a fractured bone.

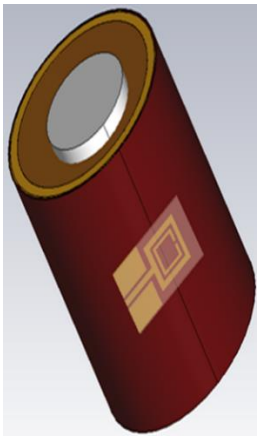

Figure 3. The RF sensor is mounted on the Bone tissues.

Table 3. A table showing the Dielectric Properties of all body Tissues used in the Bone Phantom Design.

Tissue	**Thickness (mm)**	**Conductivity (S/m)**	**Relative Permittivity**
Skin	1	5.82	3.32
Fat average	7.5	1.28	9.28
Muscle	25	7.80	4.44
Bone cortical (average)	35	1.68	8.79
Hematoma (blood)	1	9.87	4.86

5. Signal Processing in Frequency Domain

This research is conducted to determine the depth of fracture in a human bone based on the variations in the dielectric properties of the underlying tissues. To characterise the nature of these tissues, a monostatic radar configuration was used in our microwave detection system. The reflective coefficient of the antenna was measured in free space to validate the efficiency of the antenna, and the most reactive part of the antenna was determined through the E-field magnitude as shown in Figure 4 to help predict the best position and direction suitable for moving the antenna around the body surface under investigation. S-Parameter is frequency-dependent, making it suitable for the analysis of the processed signals in the frequency domain. Therefore, calculating the S – Parameter, a reflection coefficient for a one-port network was used in the equations below.

$$Z_{in} = Z_0 \frac{1 + S_{11}}{1 - S_{11}}$$

where Z_{in} represents the input impedance,

Z_0= 50Ω which represents the characteristics of impedance,

S_{11} directly relates to the voltage and current through the input impedance of the port.

6. Experimental Results

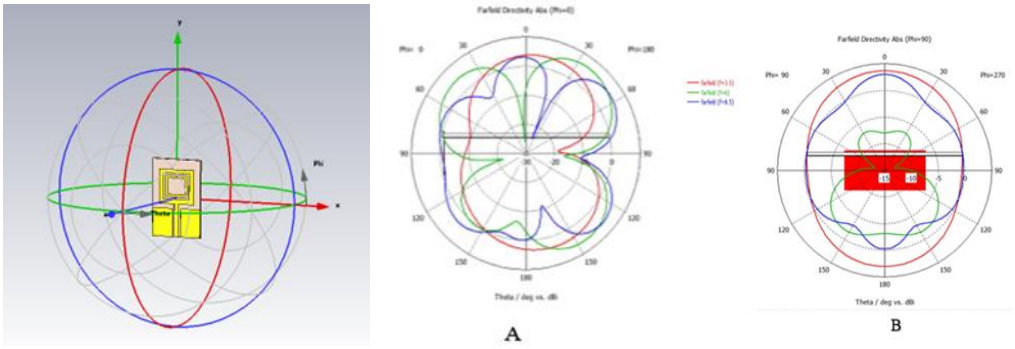

Figure 4. Omnidirectional antenna and far-field directivity of the antenna.

Figure 4 shows all the radiation zones of the antenna where a stable electromagnetic field pattern is produced by the selected antenna. From the image, there is an indication of a stable radiation pattern experienced at all sides of the antenna, making the antenna a good fit for the investigation. At these fields, no significant change or instability is felt at the receiving end of the antenna. Figure 4A depicts the directivity at Phi=0 and the Figure 4B indicates the directivity at Phi 90. Figure 4 suggests the angle at which the electromagnetic field of the antenna is most felt when positioned. Each colour code represents the frequency at which the electromagnetic

radiation emanating from the antenna travels. Red represents the 1GHz, the Green represents 6 GHz, and the Blue represents the 3 GHz. These coloured maps depict the extent of travel of the electromagnetic radiations propagated by the antenna when positioned at Phi=0° and Phi=90° as shown in **A** and **B** respectively.

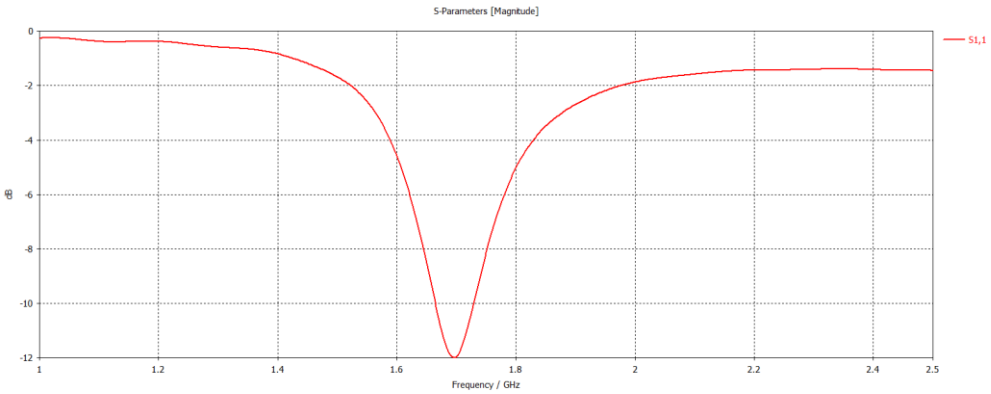

Figure 5. A Graph of S - Parameter depicting the actual bandwidth of the antenna when tested in free space.

Figure 5 shows how wide the bandwidth of the designed antenna is when tested in the frequency domain of 1-3 GHz. This is proof of the concept that the antenna designed can operate in a higher bandwidth as shown at -10 dB as shown on the graph. That is, at -10 dB, the antenna attains its highest bandwidth when tested in free space or in the absence of any body tissue capable of interfering with the radiation propagation due to the presence of their dielectric features.

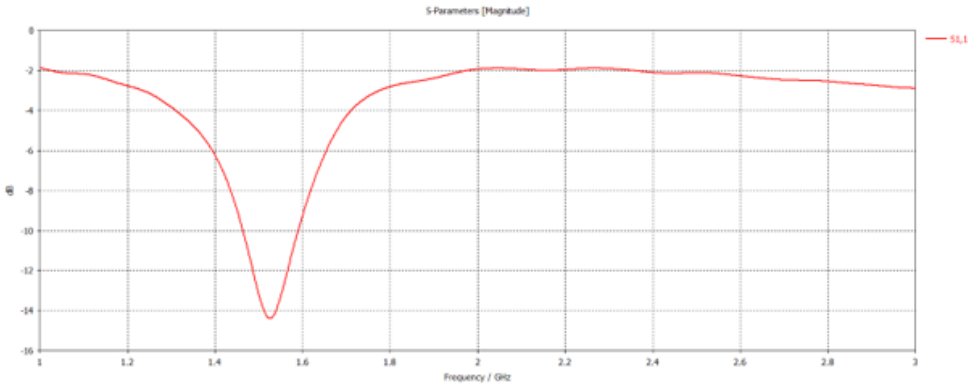

Figure 6. A Graph of S - Parameter depicting the actual bandwidth of the antenna when tested on the bone phantom *Without fracture.*

The S-parameter in Figures 6 and 7 was taken when the antenna was tested in the frequency domain of 3.5 – 8.5 GHz. The graph shows a great deviation as compared to that of Figure 6

when the same antenna was tested in free space. This shows a reduction in the flow or propagation of the voltage through the input impedance of the port. A lower magnitude is observed as compared to the antenna tested in free space.

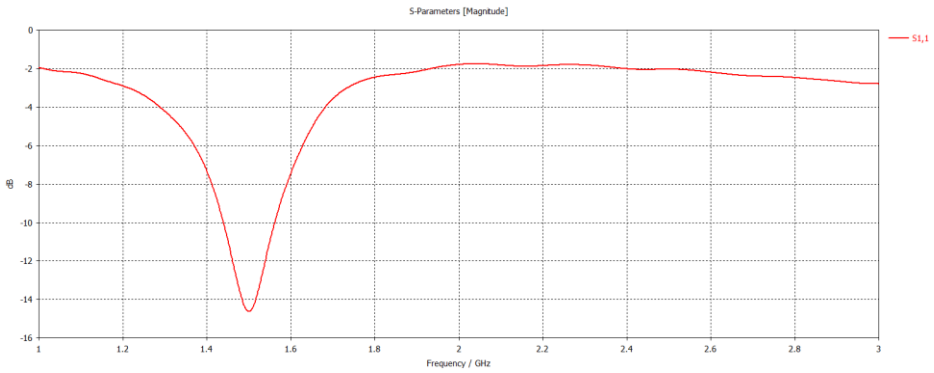

Figure 7. A Graph of S-Parameter depicting the actual bandwidth of the antenna when tested the bone phantom with a *Fracture Depth of 2mm*.

The magnitude of Figure 7 above is lower than that of Figure 6. This deviation may be attributed to the presence of the 1mm fracture which has introduced blood as part of the tissues present in the phantom. An increase in the distortion of the radiation propagation was observed due to the dielectric properties of the hematoma (blood) present in the fractured region.

7. Conclusions

In this research, bone fracture detection at different fracture depths was investigated using a microwave imaging technique. A variation in the S-parameter (magnitude against frequency) was observed in antenna propagation at a frequency range of 3.5 – 8.5 GHz in free space, attached to bone phantom without fracture, and fractures of 1mm, 2mm, and 5mm. The free space results were observed to be the best magnitude and frequency bandwidth and the fracture depth of 5mm showed the least magnitude with frequency bandwidth. The results obtained confirm that indeed a microwave sensor can be applied in the medical imaging and diagnosis of human fractures and further differentiate the extent or depth of fracture as a way of closely studying the patterns of the healing process.

Acknowledgement. This work is partially supported by the innovation programme under grant agreement H2020-MSCA-RISE-2022-2027 (ID: 101086492), Marie Skłodowska-Curie, Research and Innovation Staff Exchange (RISE), and the financial support from the UK Engineering and Physical Sciences Research Council (EPSRC) under grant EP/X039366/1

References

[1] Meena, T. and Roy, S. (2022). Bone Fracture Detection Using Deep Supervised Learning from Radiological Images: A Paradigm Shift. *Diagnostics*, 12(10), p.2420. doi:https://doi.org/10.3390/diagnostics12102420.

[2] Palm, H.-G., Lang, P., Hackenbroch, C., Sailer, L. and Friemert, B. (2019). Dual-energy CT as an innovative method for diagnosing fragility fractures of the pelvic ring: a retrospective comparison with MRI as the gold standard. *Archives of Orthopaedic and Trauma Surgery*, 140(4), pp.473–480. doi:https://doi.org/10.1007/s00402-019-03283-8.

[3] Upadhyay, R.S. and Tanwar, P. (2019). *A Review on Bone Fracture Detection Techniques using Image Processing*. [online] IEEE Xplore. doi:https://doi.org/10.1109/ICCS45141.2019.9065874.

[4] Felicio, J.M., Bioucas-Dias, J.M., Costa, J.R. and Fernandes, C.A. (2020). Microwave Breast Imaging Using a Dry Setup. *IEEE Transactions on Computational Imaging*, 6, pp.167–180. doi:https://doi.org/10.1109/tci.2019.2931079.

[5] Santos, K.C., Fernandes, C.A. and Costa, J.R. (2022). Feasibility of Bone Fracture Detection Using Microwave Imaging. *IEEE Open Journal of Antennas and Propagation*, [online] 3, pp.836–847. doi:https://doi.org/10.1109/OJAP.2022.3194217.

[6] Mustafa, S., Mohammed, B. and Abbosh, A. (2013). Novel Preprocessing Techniques for Accurate Microwave Imaging of Human Brain. *IEEE Antennas and Wireless Propagation Letters*, 12, pp.460–463. doi:https://doi.org/10.1109/lawp.2013.2255095.

[7] Tobon Vasquez, J.A., Scapaticci, R., Turvani, G., Bellizzi, G., Rodriguez-Duarte, D.O., Joachimowicz, N., Duchêne, B., Tedeschi, E., Casu, M.R., Crocco, L. and Vipiana, F. (2020). A Prototype Microwave System for 3D Brain Stroke Imaging. *Sensors*, [online] 20(9), p.2607. doi:https://doi.org/10.3390/s20092607.

[8] Khalesi, B., Sohani, B., Ghavami, N., Ghavami, M., Dudley, S. and Tiberi, G. (2020). Free-Space Operating Microwave Imaging Device for Bone Lesion Detection: A Phantom Investigation. *IEEE Antennas and Wireless Propagation Letters*, 19(12), pp.2393–2397. doi:https://doi.org/10.1109/lawp.2020.3034039.

[9] Khalid, B., Khalesi, B., Ghavami, N., Sani, L., Vispa, A., Badia, M., Dudley, S., Ghavami, M. and Tiberi, G. (2022). 3D Huygens Principle Based Microwave Imaging Through MammoWave Device: Validation Through Phantoms. *IEEE Access*, 10, pp.106770–106780. doi:https://doi.org/10.1109/access.2022.3211957.

[10] O'Loughlin, D., O'Halloran, M., Moloney, B.M., Glavin, M., Jones, E. and Elahi, M.A. (2018). Microwave Breast Imaging: Clinical Advances and Remaining Challenges. IEEE Transactions on Biomedical Engineering, 65(11), pp.2580–2590. doi:https://doi.org/10.1109/tbme.2018.2809541.

[11] Santos, K.C., Fernandes, Carlos.A. and Costa, J.R. (2021). A study on the sensitivity of microwave imaging for detecting small-width bone fractures. [online] IEEE Xplore. doi:https://doi.org/10.23919/EuCAP51087.2021.9411065.

[12] Vimal Samsingh Ramalingam, Malathi Kanagasabai and Esther Florence Sundarsingh (2019). A Compact Microwave Device for Fracture Diagnosis of the Human Tibia. *IEEE Transactions on Components, Packaging and Manufacturing Technology*, 9(4), pp.661–668. doi:https://doi.org/10.1109/tcpmt.2019.2893367.

[13] C. Santos, K., A. Fernandes, Carlos. and R. Costa, J. (2022). Experimental Evaluation of Thin Bone Fracture Detection Using Microwave Imaging. [online] ieeexplore.ieee.org. Available at: https://ieeexplore.ieee.org/document/9769388 [Accessed 18 Oct. 2023].

[14] D. Perez, M., Mohd Shah, S.R., Velander, J. and Raaben, M. (2017). *Microwave Sensors for New Approach in Monitoring Hip Fracture Healing*. [online] ieeexplore.ieee.org. Available at: https://ieeexplore.ieee.org/document/7928698 [Accessed 11 Oct. 2023].

[15] Nouri Moqadam, A. and Kazemi, R. (2023). Design of a novel dual-polarized microwave sensor for human bone fracture detection using reactive impedance surfaces. Scientific Reports, [online] 13(1), p.10776. doi:https://doi.org/10.1038/s41598-023-38039-3.